2007 International Symposium on Nonlinear Theory and its Applications
NOLTA'07, Vancouver, Canada, September 16-19, 2007

DT-CNN Based Resolution Enhancement of Images using Cycle Spinning

Takefumi Konishi*, Tsuyoshi Otake*, Hisashi Aomori†,
Nobuaki Takahashi‡ and Mamoru Tanaka†

* Department of Media-Network Science, Tamagawa University,
6-1-1, Tamagawagakuen, Machida-shi, Tokyo, 194-8610 Japan
† Department of Electrical and Electronics Engineering, Sophia University,
7-1, Kioi-cho, Chiyoda-ku, Tokyo, 102-8554 Japan
‡ IBM Technology Collaboration Solutions, IBM Japan, Ltd.,
1623-14, Shimotsuruma, Yamato-shi, Kanagawa, 242-8502 Japan
Email: knsta1ec@engs.tamagawa.ac.jp

Abstract—In this paper, novel image resolution enhancement technique using discrete-time celluar neural network (DT-CNN) with cycle spinning is proposed. Generally, interpolated images include a lot of noises when the enhacement factor is large. The denoising process is necessary to supress such noises. In our proposed method, images are interpolated by exploiting the nonlinear interpolative dynamics of the DT-CNN with a feedback A-template using cycle spinning. The experimental evaluation shows that the proposed method produces better results than those of the conventional image resolution enhancement methods.

1. Introduction

Image resolution enhancement and interpolation are used to generate a high-resolution (HR) image from its low-resolution (LR) version. It is very important technique for high-resolution image processing applications such as digital HDTV, digital photogrammetry, high-quality printing, medical imaging, military purpose imaging, and so on. Recently wavelet based interpolation methods are discussed in many literatures [1]-[4]. In wavelet based techniques, it is assumed that the LR image to be resolution enhanced is the lowpass-filtered and down-sampled HR image. These methods are based on wavelet-domain zero padding (WZP) [3][4]. In the WZP, the LR image values are set to low-frequency subband of wavelet transform and the high-frequency subbands are composed of all-zero. Therefore, due to the constraint of the dyadic decomposition for wavelet transform, its resolution enhancement factor is limited to 2^n, $(n = 1, 2, ...)$.

In general, it is issue for image interpolation that the reconstructed image exhibits some visual artifacts. When a signal contains several discontinuities in neighborhood, the cycle spinning, which apply a range of shifts and average over the several results, is a suitable method to suppress such artifacts. Cycle spinning has been shown to be successful toward image resolution enhancement in the wavelet domain [4].

In this paper, we propose an image resolution enhancement technique with arbitrary enhancement parameters using a discrete-time cellular neural network (DT-CNN) and the cycle spinning. The DT-CNN has been applied to many applications such as image compression, filtering and recognition [5]-[11]. The nonlinear interpolative dynamics by feedback A-template is one of the significant characteristics of CNN, and it is a solver to solve the optimization problem to minimize the Lyapunov energy function. In our proposed method, the interpolation is based on the dynamics of the DT-CNN, where the output function is utilized in order to consider the nonlinear quantization error for optimization. At the equilibrium state of the DT-CNN, we can obtain the optimal coefficients to be established an optimal prediction image. In order to obtain an optimal interpolated image, we introduce the principle of the cycle spinning technique to the nonlinear interpolative dynamics of the DT-CNN.

2. Cycle Spinning

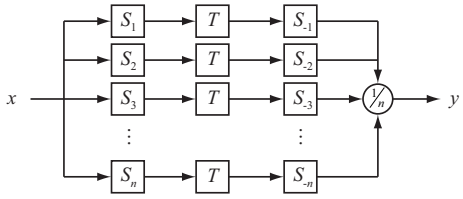

Figure 1: Cycle spinning.

Figure 1 shows the block diagram of the cycle spinning. The cycle spinning considers a range of shifts and set

$$y = \text{Ave } S_{-h}(T(S_h(x))), \qquad h \in H \tag{1}$$

where x is an input signal, y is an output signal, S_h is a shift operator, S_{-h} is an unshift operator and T is an analysis technique. H and h are range of shifts and shift value respectively. The cycle spinning first shifts the data, denoises the shifted data, and then unshifts the denoised data. Doing this for each of a range of shifts, and averaging the several results, the effective denoised signal data is obtained.

3. Image Resolution Enhancement using DT-CNN with Cycle Spinning

3.1. DT-CNN

Figure 2 shows the block diagram of DT-CNN. The state equation of the DT-CNN is described in matrix form as

$$\mathbf{x}_{n+1} = \mathbf{A}\mathbf{f}(\mathbf{x}_n) + \mathbf{B}\mathbf{u} + \mathbf{T}, \tag{2}$$

where $\mathbf{u}$ is an input vector, $\mathbf{x}$ is a state variable, $\mathbf{f}()$ is a multi-level quantizing function, $\mathbf{A}$ and $\mathbf{B}$ are feedback and feedforward template matrices, respectively, and $\mathbf{T}$ is a constant vector. Let $\mathbf{y} = \mathbf{f}(\mathbf{x})$, then the Lyapunov energy function E of the DT-CNN is defined by

$$E = -\frac{1}{2}\mathbf{y}^t(\mathbf{A} - \delta\mathbf{I})\mathbf{y} - \mathbf{y}^t\mathbf{B}\mathbf{u} - \mathbf{T}^t\mathbf{y}, \tag{3}$$

where δ is a positive constant value to determine the quantizing region. If the $\mathbf{A}$ matrix is symmetric and its diagonal elements are larger than zero, it is proved that the Lyapunov energy function becomes a monotone decreasing function [12][13].

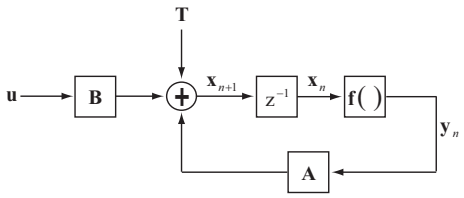

Figure 2: Discrete-time cellular neural network.

3.2. Image Resolution Enhancement using Two-Layered DT-CNN with Cycle Spinning

In the proposed method, images are interpolated using the two-layered DT-CNN. At the first layer DT-CNN, in order to obtain the high accuracy prediction images, it is necessary that the image can be reconstructed based on the distortion defined by

$$\mathrm{dist}(\mathbf{y}, \mathbf{u}) = \frac{1}{2}\mathbf{y}^t(\mathbf{G}\mathbf{y} - \mathbf{u}), \tag{4}$$

where $\mathbf{G}$ is a Gaussian filter. This distortion means that the difference between the interpolative predicted image and the input image should be small. By the comparison between equation (3) and (4), the A-template, B-template, and the constant T can be determined as

$$\mathbf{A} = A(i, j; k, l), \qquad C(k, l) \in N_r(i, j) \tag{5}$$

$$= \begin{cases} -\dfrac{1}{2\pi\sigma^2} + \lambda \\ \qquad \text{if } k = i \text{ and } l = j, \\ -\dfrac{1}{2\pi\sigma^2}\exp\left(-\dfrac{\{(k-i)^2 + (l-j)^2\}}{2\sigma^2}\right) \\ \qquad \text{otherwise,} \end{cases}$$

$$\mathbf{B} = B(i, j; k, l), \qquad C(k, l) \in N_r(i, j) \tag{6}$$

$$= \begin{cases} 1 & \text{if } k = i \text{ and } l = j, \\ 0 & \text{otherwise.} \end{cases}$$

$$T = 0 \tag{7}$$

where σ is the standard deviation of Gaussian function and λ is a regularization parameter. The B-template is only nonzero at the center value. Applying the principle of cycle spinning to first layer DT-CNN, we represent the dynamics of DT-CNN using above parameters as follows:

$$x_{ij}(t+1) = \text{Ave}\ \ S_{-d}\left(\sum_{C(k,l)\in N_r(i,j)} S_d(A(i, j; k, l))y_{kl}(t) + u_{kl}\right), \tag{8}$$

$$y_{ij}(t+1) = f(x_{ij}(t+1)), \tag{9}$$

where $N_r(i, j)$ is the r-neighborhood of cell $C(i, j)$ as $N_r(i, j) = \{C(k, l) | \max\{|k - i|, |l - j|\} \le r\}$. $x_{ij}(t)$ is an internal state, $y_{ij}(t)$ is an output of cell and u_{ij} is an input of cell $C(i, j)$. S_d is a shift operator applying horizontal and vertical shifts of (k, l) for $(k - d, l)$, $(k + d, l)$, (k, l), $(k, l - d)$ and $(k, l + d)$ as shown in Figure 4. S_{-d} is an unshift operator and d is a shift value of operater. These operators are meaning that the center point of the A-template shifts to each point of operator, and then averaging over the each unshifted convolution results of shifted A-template. The output function $f()$ corresponds to the rounding operator. The output function plays an important role that the interpolation is optimized considering the nonlinearity caused by quantization noises. The input image pixels are set to u_{ij} and the equilibrium output y^e_{ij} is obtained after the transition of the network.

Next, the output of the first layer DT-CNN becomes the input of the second layer DT-CNN which has no dynamics. The output of the second layer DT-CNN provides the denoised predicted values. The image enhancement is composed of the horizontal and vertical processes illustrated in Figure 5. At the horizontal resolution enhancement stage, the pixel with coordinates (i, j) of the input image is mapped to pixel (i', j) of the resolution enhancement image. Let d_m be an enlargement parameter, the relationship between the pixel (i, j) and (i', j) is determined as $(i', j) = (id_m, j)$. As shown in Figure 6, the deficient pixel with coordinates (k, l) of the enlarged image is obtained by

$$\hat{y}_{i'j} = \text{Ave}\ \ S_{-d'}\left(\sum_{y_{kl}\in N'_h(i',j)} S_{d'}(\hat{B}_h(i', j; k, l))y^e_{i'j}\right), \tag{10}$$

where $S_{d'}$ is a shift operator and $S_{-d'}$ is an unshift operator. At the second layer of horizontal stage, a range of shift operator is defined by extending range of first layer shift operator horizontally, that is $(k - d')$, $(k + d')$, (k, l), $(k, l - d)$ and $(k, l + d)$. The relationship between d and d'

is determined as $d' = d \cdot d_m$. $\hat{\mathrm{B}}_{\mathrm{h}}$-template can be calculated by extending A-template of the first layer DT-CNN horizontally, that is

$$\hat{\mathbf{B}}_{\mathbf{h}} = \hat{B}_h(i', j; k, l), \qquad C(k,l) \in N'_h(i', j) \quad (11)$$
$$= \frac{1}{2\pi\sigma^2}\exp\left(-\frac{(k-i')^2/d_m^2 + (l-j)^2}{2\sigma^2}\right),$$
$$N'_h(i', j) = \{C(k,l) \| k - i' | \le r d_m, |l - j| \le r\}.$$

In the same manner, at the vertical resolution enhancement stage, the pixel (i, j) is mapped to the pixel $(i, j') = (i, jd_m)$, and enlarged image is obtained by

$$\hat{y}_{ij'} = \text{Ave}\ \ S_{-d'}\left(\sum_{y_{kl} \in N'_v(i,j')} S_{d'}(\hat{B}_v(i, j'; k, l)) y^e_{ij'}\right), \quad (12)$$

where a range of shift is redefined as $(k-d, l)$, $(k+d, l)$, (k, l), $(k, l-d')$ and $(k, l+d')$. $\hat{\mathrm{B}}_{\mathrm{v}}$-template is derived by

$$\hat{\mathbf{B}}_{\mathbf{v}} = \hat{B}_v(i, j'; k, l), \qquad C(k,l) \in N'_v(i, j') \quad (13)$$
$$= \frac{1}{2\pi\sigma^2}\exp\left(-\frac{(k-i)^2 + (l-j')^2/d_m^2}{2\sigma^2}\right),$$
$$N'_v(i, j') = \{C(k,l) \| k - i | \le r, |l - j'| \le r d_m\}.$$

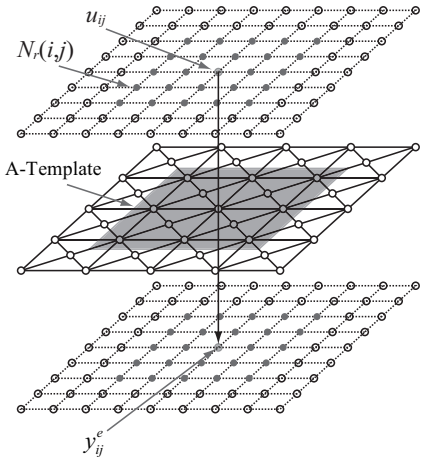

Figure 3: First layer DT-CNN.

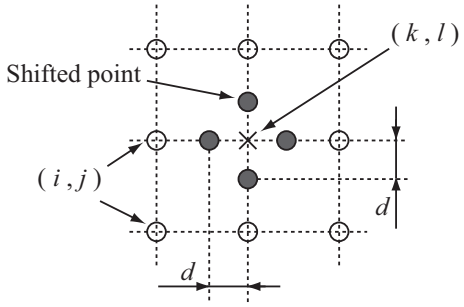

Figure 4: Shift operator of cycle spinning.

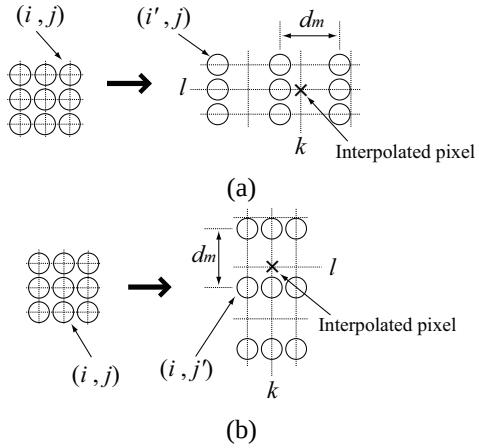

Figure 5: Image enlargement of each stage. (a) horizontal enlargement and (b) vertical enlargement.

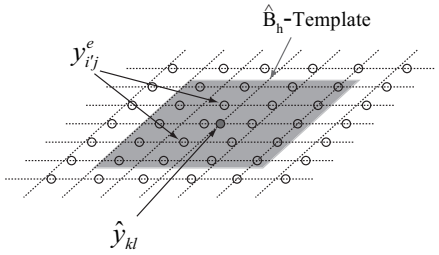

Figure 6: Second layer DT-CNN.

4. Experimental Results

We evaluated the effectiveness of our proposed image resolution enhancement method using the two-layered DT-CNN with cycle spinning. We applied our method to the 8-bit gray-scale standard test images; "Aerial," "Airfield," "Boat," "Couple," "Crowd," "Lena," "Sailboat," and "Tiffany." These were lowpass filtered and downsampled to provide the LR images available for images enhancement. The performance of the proposed method was compared with that of the bicubic interpolation algorithm which is indicated as "BC" and the wavelet interpolation algorithm based on WZP using the well-known Le Gall 5/3 tap filter which is indicated as "WT." For the simulation, the parameters were decided experimentally; the standard deviation of Gaussian σ=0.54, the r-neighborhood of cell r=2, the regularization parameter $\lambda = 1/2\pi\sigma^2$. The enlargement parameter d_m must be limited to 2^n, $(n = 1, 2, ...)$ for WZP. Therefore, d_m was set to 2 in order to compare with the performance of WT.

Table 1 shows the results of peak signal-to-noise ratio (PSNR) values between the original image and the resolution enhanced image. The proposed method outperforms BC, and has better and competitive performance compared with WT.

Next, we estimated the performance with arbitrary enhancement parameter. Test images were resized from

512×512 to 200×200 and 300×300 by BC, then, image resolution enhancement methods were applied ($d_m = 2.56$ and $d_m \approx 1.71$). As shown in Table 2, the performance of the proposed method has better results than BC for most cases.

Table 1: PSNR of resolution enhanced images (from 256×256 to 512×512)

Image	WT	BC	Proposed
Aerial	27.797	27.442	**28.137**
Airfield	27.058	27.06	**27.315**
Boat	30.322	30.184	**30.518**
Couple	30.076	29.979	**30.285**
Crowd	33.043	32.943	**33.740**
Lena	34.513	34.388	**34.983**
SailBoat	30.293	29.358	**30.503**
Tiffany	**30.740**	30.344	30.083

Table 2: PSNR of resolution enhanced images (from 200×200 and 300×300 to 512×512)

Image	200×200		300×300	
	BC	Proposed	BC	Proposed
Aerial	24.260	**24.815**	28.671	**29.490**
Airfield	23.882	**24.291**	27.921	**28.273**
Boat	26.952	**27.360**	30.891	**31.233**
Couple	26.509	**26.916**	31.077	**31.417**
Crowd	29.513	**30.034**	34.717	**35.397**
Lena	31.229	**31.630**	35.700	**36.196**
SailBoat	25.937	**27.270**	30.137	**31.360**
Tiffany	26.952	**28.125**	**30.978**	30.682

5. Conclusion

The image resolution enhancement method using two-layered DT-CNN with cycle spinning was proposed. Our proposed method makes good use of the nonlinear interpolative effect of DT-CNN to obtain an enhanced resolution image. The principle of the cycle spinning for denoising was adapted to the nonlinear interpolative dynamics of DT-CNN. The experimental results show that our proposed method outperforms the bicubic interpolation and has better and competitive performances compared with conventional wavelet based resolution enhancement method.

References

[1] S. G. Chang, Z. Cvetkovic and M. Vetterli, "Resolution enhancement of images using wavelet transform extrema extrapolation," Proc. ICASSP95, vol. 4, pp. 2379-2382, 1995.

[2] W. K. Carey, D. B. Chuang and S. S. Hemami, "Regularity-preserving image interpolation," IEEE Trans. Image Process., vol. 9, no. 8, pp. 1295-1297, 1999.

[3] A. Temizel and T. Vlachos, "Wavelet domain image resolution enhancement using cycle-spinning," Electronics Letters, vol. 41, no. 3, 2005.

[4] A. Temizel and T. Vlachos, "Image resolution upscaling in the wavelet domain using directional cycle spinning," Journal of Electronic Imaging, vol. 14, no. 4, pp. 040501-1 - 040501-3, 2005.

[5] L. O. Chua and L. Yang, "Cellular neural networks: Theory," IEEE Trans. Circuits Syst., vol. 35, no. 10, pp. 1257-1272, 1988.

[6] L. O. Chua and T. Roska, "The CNN paradigm," IEEE Trans. Circuits Syst., vol. 40, no. 3, pp. 147-156, 1993.

[7] M. Ikegami and M. Tanaka, "Image coding and decoding by discrete time cellular neural networks and its error evaluation," IEICE Trans. Fundamentals (Japanese Edition), vol. J77-A, no. 7, pp. 954-964, 1994.

[8] K. R. Crounse and L. O. Chua, "Methods for image processing and pattern formation in cellular neural networks: A tutorial," IEEE Trans. Circuits Syst., vol. 43, no. 10, pp. 583-601, 1995.

[9] M. Balsi and S. David, "Cellular neural networks for image compression by adaptive morphological subband coding," Proc. IEEE ECCTD 97, pp. 634-638, 1997.

[10] P. L. Venetianer and T. Roska, "Image compression by cellular neural networks," IEEE Trans. Circuits Syst., vol. 45, no. 3, pp. 205-215, 1998.

[11] M. Tanaka, Y. Tanji, M. Ohnishi and T. Nakaguchi, "Lossless image compression and reconstruction by cellular neural networks," Proc. IEEE CNNA2000, 2000.

[12] N. Takahashi, T. Otake and M. Tanaka, "Nonlinear interpolative effect of feedback template for image processing by discrete-time cellular neural network," J. Circuit Syst. Comp., vol. 12, no. 4, pp. 505-518, 2003.

[13] H. Aomori, K. Kawakami, T. Otake, N. Takahashi, M. Yamauchi and M. Tanaka, "Separable 2D Lifting Using Discrete-Time Cellular Neural Networks for Lossless Image Coding," IEICE Trans. Fundamentals, vol. E88-A, no. 10, pp. 2607-2614, 2005.